Full Text View

Volume 32, Issue 12 (December 2002)

Journal of Physical Oceanography
Article: pp. 3551–3561 | Abstract | PDF (272K)

A Theory of Equatorial Deep Jets*

Joseph Pedlosky

Woods Hole Oceanographic Institution, Woods Hole, Massachusetts

(Manuscript received December 14, 2001, in final form June 13, 2002)

DOI: 10.1175/1520-0485(2002)032<3551:ATOEDJ>2.0.CO;2

ABSTRACT

A simple linear theory of the circulation in a meridionally bounded equatorial ocean driven by density mixing localized near the eastern boundary is used to model the subthermocline circulation of the equatorial oceans. The mixing is modeled by a specified, spatially limited source term in the density equation. The theory is for a steady circulation, and the model, which is continuously stratified, contains simple linear drag laws for frictional dissipation and a similar, linear damping for density anomalies. The model employs Gill's formulation of the basic linear equations near the equator. The satisfaction of the condition of zero zonal flow at both bounding meridians requires the determination of the amplitude of the Kelvin component (or its steady counterpart) by an integral condition over the domain of the flow. When that condition is satisfied, the solution, for reasonable settings of the parameters, naturally yields an alternating array of zonal currents localized within a deformation radius of the equator. An essential condition for the appearance of this high vertical mode zonal structure is the localization of the forcing to the eastern boundary and to a small vertical region at the top of the domain, which is identified with the mixing occurring at the base of the equatorial thermocline.

1. Introduction

The discovery of alternating zonal currents at the equator, first in the Indian Ocean by Luyten and Swallow (1976) and their subsequent observation in both the Pacific and the Atlantic (see, e.g., O'Neill and Luyten 1984; Firing 1987; and Ponte et al. 1990), poses an extremely intriguing dynamical puzzle. The short vertical scale of the observed jets, about 100–300 m, and their moderate velocities (on the order of 20 cm s^{-1} or less) initially encouraged their identification as an equatorial wave response to forcing in the equatorial band on long timescales (see, e.g., the discussion in O'Neil and Luyten). Early theoretical attempts to explain the deep jets as a forced wave response to surface input (e.g., Wunsch 1977) were frustrated by the shallow angle of descent of energy pathways at the low frequencies required to obtain realistic vertical scales. In an ocean of finite longitudinal extent it is difficult to so explain the emergence of energy at great depths. Attempts have also been made to explain the jets as a consequence of time dependent forcing at the boundaries. Ponte (1989), for example, specifies the structure of the zonal velocity at either an eastern or western equatorial boundary and computes the interior structure. In such cases however, the vertical structure of the solution, in particular, the vertical wavenumber of the oscillating current, is completely specified as a boundary condition and this frustrates an attempt to explain the structure of the current as a response to external forcing.

In this paper I present a model for the equatorial deep jets which is fundamentally based on the linear, steady equatorial model introduced by Gill (1980) and Anderson and Rowlands (1976; in particular see Gill 1982, his section 11.4). Similar investigations of the steady problem date to the pioneering work of McCreary (1981) who attempted a linear steady model for the Equatorial Undercurrent. More recently Wang et al. (1994) described a model driven by a specified zonal inflow within the equatorial region at the depth of the observed deep jets. Although yielding plausible structures, there is no explanation for the mechanism that produces this western boundary forcing.

The inclusion of both eastern and western boundaries to the domain adds elements of particular subtlety. The zonal velocity is forced to vanish at both boundaries in this model and it is assumed, and verified post hoc, that all solutions decay for increasing latitude so that the domain of motion is limited. The model is driven by an inhomogeneous forcing term in the equation for the density field and it is suggested that this represents the effects of turbulent mixing which is observed to occur at the base of the equatorial thermocline. There have been several studies of the distribution of thermocline mixing in the upper equatorial ocean. One of the most complete is the recent study of Sloyan et al. (2002, manuscript submitted to *J. Phys. Oceanogr.*). This study shows rather intense diapycnal velocities at and below the base of the thermocline in the eastern boundary region of the Pacific especially east of 95°W. In the theory to be presented that mixing enters as a forcing term for the equatorial density field and is spatially limited.

It is particularly important to the theory that this forcing be limited in its zonal extent and its vertical range. The mixing exponentially decays away from both the eastern boundary and the upper surface, taken here to represent the base of the thermocline. It is important to note that such a forcing does not impose the vertical scale for the deep jets nor does it locally force the flow except near the boundary.

The forcing excites the steady equivalent of the whole class of equatorial wave modes, the amplitudes of which are determined by the forcing, the boundary conditions on the zonal flow and the integral condition of mass conservation. In particular, these conditions set the amplitudes of the steady equivalent Kelvin modes that are seen to dominate the solution. A parameter range is chosen that would allow the lowest few free Kelvin waves to transit the basin but strongly thermally damps the higher modes. In this case the steady response consists of a sequence of equatorial zonal jets whose vertical wavenumber depends of the ratio of the transit time to the damping timescale. The longer the damping time the smaller is the vertical wavelength of the zonal jet response. For strong thermal damping the forced signal would not exit the forcing region. For extremely weak thermal damping the solution responds in a Sverdrup type response in which the motion is limited to the depth of the forcing. Deep jets occur over a range of thermal damping coefficient intermediate to these two extremes.

Section 2 describes the formulation of the basic model. Section 3 outlines the analysis in terms of vertical and meridional modes and describes the determination of the solution in response to the boundary conditions. Section 4 describes the integral condition and closes the problem. In section 5, I present the principal results of the calculation, and section 6 concludes with summary and discussion of the results.

There is no question that the linearity of the proposed model and the specification a priori of the density mixing are the weakest points of the theory. It is offered as a simple explanation for an intriguing and perplexing phenomenon and, it is hoped, the basis for more complete modeling.

2. Formulation

The model used in this study is, fundamentally, the model first introduced by Gill and discussed at length in his text (Gill 1982). The ocean model is centered at the equator and is bounded at $x = 0$ and $x = L$ by meridional walls. The fluid's vertical domain is $-H < z < 0$. The system of linearized momentum and density equations, supplemented by the continuity equation is

$$Du - fv = -P_x \qquad (2.1a)$$

$$Dv + fu = -P_y \qquad (2.1b)$$

$$P_z = -bg \qquad (2.1c)$$

$$u_x + v_y + w_z = 0 \qquad (2.1d)$$

$$Db - wN^2/g = -Q, \qquad (2.1e)$$

where the operator D is defined as

$$D \equiv \frac{\partial}{\partial t} + \kappa, \qquad (2.2)$$

where κ is both the Rayleigh friction drag inverse timescale as well as the scale for linear damping of density anomalies and it is the latter that is most crucial for the structure of the response. Here, N is the buoyancy frequency while b is the ratio of the density anomaly to the background density, and P is the pressure divided by the background density in the

Boussinesq approximation. The Coriolis parameter in the equatorial beta plane approximation is $f = \beta y$. We consider the region unbounded in y but the solutions will be naturally limited to a finite region in y.

The function Q is the forcing in our model. Positive Q represents a reduction in density; one might think of it as representing the entrainment of lighter fluid from the thermocline into the deeper ocean by mixing. It thus represents a source of buoyancy and is meant to stand in for mixing of the fluid by processes unresolved in the model but present in observations of equatorial mixing as described in the introduction. It will be limited to a region near the eastern boundary and to a narrow zone at the top of the fluid at $z = 0$ which we identify with the base of the equatorial thermocline. In the present model the buoyancy frequency N will be taken to be constant. This condition can be easily relaxed but it is simpler to consider N constant and little is gained by using more realistic buoyancy profiles. The simplicity of the theory does not really justify such attempts at detailed realism.

The appropriate boundary conditions for our model are

$$u = 0, \qquad x = 0, L \tag{2.3a}$$

$$w = 0, \qquad z = 0, -H. \tag{2.3b}$$

With constant buoyancy frequency, and with the boundary conditions (2.3b) it is convenient to represent the solution as a Fourier series in z, namely,

$$(u, v, P) = \sum_{n=1} (u_n, v_n, g\eta_n) \cos(n\pi z/H) \tag{2.4a}$$

$$w = \sum_{n=1} w_n \sin(n\pi z/H). \tag{2.4b}$$

Note that the sums for the horizontal velocity start with $n = 1$. The barotropic response ($n = 0$) to pure buoyancy forcing in this linear model is identically zero as can be easily shown. After projecting (2.2) on the appropriate Fourier functions, eliminating the density between the density and hydrostatic equations and using the continuity equation, the resulting equations for the amplitudes are

$$Du - fv = -g\eta_x \tag{2.5a}$$

$$Dv + fu = -g\eta_y \tag{2.5b}$$

$$D\eta + h(u_x + v_y) = -E \tag{2.5c}$$

$$E(n) = \frac{2}{n\pi} \int_{-H}^{0} Q \sin\left(\frac{n\pi z}{H}\right) dz. \tag{2.5d}$$

In the above equations, the subscript n on each amplitude has been suppressed for typographic clarity. That suppressed index is, of course, implicitly present and used when reconstructing the total solution. The constant $h(n)$ is the equivalent depth for the nth mode and is, for the case of constant N,

$$h(n) = \frac{N^2H^2}{gn^2\pi^2} \tag{2.6}$$

corresponding to gravity wave speeds

$$c = c(n) = [gh(n)]^{1/2} = \frac{NH}{n\pi} = \frac{c(1)}{n}. \tag{2.7}$$

Following Gill (1982) it is useful to introduce the variables

$$q = g\eta/c + u, \tag{2.8a}$$

$$r = g\eta/c - u, \tag{2.8b}$$

in terms of which we obtain from (2.5 a,c)

$$Dr - cr_x + cv_y + fv = -cE/H. \qquad (2.9b)$$

These variables allow a convenient way to express the projection of the forcing exciting the zonal velocity.

The equation for potential vorticity

$$D(\zeta - f\eta/h) + \beta v = Ef/h \quad (2.10)$$

can be used with (2.5b) to obtain

$$D(cq_y + fq) + (D^2 v - cDv_x) - \beta cv = -cEf/h, \quad (2.11)$$

while (2.5b) alone can be written as

$$(cq_y + fq) + (cr_y - fr) = -2Dv. \quad (2.12)$$

3. Analysis in meridional modes

For each vertical mode, the meridional structure of the solution is most conveniently given in terms of a series in Hermite eigenfunctions, functions defined, as in Moore and Philander (1977), as

$$\psi_j(\xi) = \frac{H_j(\xi)e^{-\xi^2/2}}{(\pi^{1/2}2^j j!)^{1/2}} \qquad \xi = \frac{y}{(c/\beta)^{1/2}}, \qquad (3.1)$$

where the H_j are the Hermite polynomials and the functions in (3.1) are orthonormal over the infinite interval $-\infty \leq y \leq \infty$. Note that the new meridional variable ξ is the meridional distance *scaled with the deformation radius for the pertinent vertical mode.*

Thus each variable is represented as a series in the eigenfunctions ψ_j:

$$(q, r, v, E) = \sum_{j=0} (q_j, r_j, E_j)\psi_j(\xi), \qquad (3.2)$$

where the amplitudes of the expansion (the j subscripted variables) are functions of x alone and, were there time dependence, functions also of time. However, in our case they are functions only of longitude.

If (2.9), (2.10), and (2.11) are projected on the eigenfunctions ψ_j the following equations result after using standard identities involving the Hermite functions. The reader is referred to any standard handbook of mathematical functions (e.g., Abramowitz and Stegun 1970) for the necessary identities. In the following, the longitude variable x has been scaled by L, the basin width, so that now $0 \leq x \leq 1$. In terms of this new variable we obtain the following equations. [A similar development can be found in Anderson and Rowlands (1976).]

For $j > 0$,

$$\frac{\partial^2 q_j}{\partial x^2} + \frac{L}{\delta_S}\frac{\partial q_j}{\partial x} - q_j\left[F(2j-1) + \left(\frac{L}{L_T}\right)^2\right]$$
$$= -\left[\frac{\partial}{\partial x} - \left(\frac{L}{L_T}\right) + (j-1)\frac{L}{\delta_S}\right]\frac{L}{h}E_j$$
$$+ \frac{L}{\delta_S}[j(j-1)]^{1/2}\frac{L}{h}E_{j-2}, \qquad (3.3)$$

and for $j \geq 0$

$$+ \frac{\delta_S}{L(j+2)} \frac{L}{h} E_{j+2} \Bigg\} \qquad (3.4)$$

while for $j = 0$, the equation governing the important lowest meridional mode for the q field is simply,

$$\frac{\partial q_o}{\partial x} + \frac{L}{L_T} q_o = -\frac{L}{h} E_o, \qquad (3.5)$$

which yields the steady equivalent of the Kelvin wave.

In the above equations there are two important length scales against which the basin width is measured. They are

$$\delta_S = \frac{\kappa}{\beta}, \qquad (3.6a)$$

$$L_T = \frac{c}{\kappa}. \qquad (3.6b)$$

The first is the Stommel boundary layer scale and we will assume that it is very small with respect to L. The second is the density decay scale and is the ratio of the Kelvin wave speed to the inverse of the dissipation time scale. Since c is a function of vertical mode number this parameter varies as a function of vertical mode. As n increases L_T decreases inversely with n. Finally, the parameter F is the square of the ratio of the basin width to the equatorial deformation radius,

$$F = \frac{\beta L^2}{c}, \qquad (3.6c)$$

and is also a function of n, increasing linearly with n. We note that $F = L^2/(\delta_s L_T)$ and we recall to the reader that the above equations hold separately for each vertical mode with mode number n.

To satisfy the condition of no zonal flow on $x = 0$ and $x = 1$, we must have

$$q_j - r_j = 0, \qquad x = 0, 1 \quad (3.7)$$

for each j.

The lowest order mode, q_o corresponds to the equatorial Kelvin mode (in the time-dependent solution) but note that to determine the $j = 0$ contribution to the zonal velocity r_o must also be determined. The mode $j = 0$ corresponds to a structure which is Gaussian in y.

We specify the forcing $E(n)$ in a particularly simple form. We note from (3.3), (3.4), and (3.5) that the forcing is amplified by the very large factor L/h and given its arbitrary nature we restrict the forcing to the lowest meridional mode, that is, Gaussian in ξ:

$$\frac{L}{h} E = B(x)\psi_o(\xi), \qquad (3.8)$$

that is, $E_j = 0, j \neq 0$.

The particular structure that is chosen for the forcing Q is

$$Q(x, y, z) = B_o e^{-\alpha(1-x)} \sum_{n=1} \frac{n\pi}{H} \frac{h_n}{L} \frac{4n^2\pi[1 + e^{-\mu}(-1)^n]\psi_o(\xi_n)}{[\mu^2 + (n-1)^2\pi^2][\mu^2 + (n+1)^2\pi^2]} \sin\left(\frac{n\pi z}{H}\right) \qquad (3.9)$$

(Click the equation graphic to enlarge/reduce size)

corresponding to a distribution of heating on the equator concentrated near the upper surface and the eastern boundary. On the equator this yields a heating with a vertical and meridional structure decaying from the upper surface (the base of the thermocline) and decaying from the eastern boundary; that is,

$$Q(x, o, z) = (J/\pi^{1/4}) e^{-\alpha(1-x)} e^{\mu z/H} \sin(\pi z/H), \quad (3.10)$$

where

$$J = \frac{h(1)}{L}\frac{\pi}{\mu H}B_o. \qquad (3.11)$$

The structure of the forcing is such that it decays sharply away from the upper surface. The assumed symmetry of E with y (i.e., ξ) implies that only terms even in j will be generated in the sums for q and r (and only odd j for v).

We also take the mixing to decay away from the eastern boundary so that it exponentially decays in a distance L/α from the eastern boundary.

This form allows particularly simple analytical solutions. For example, the solution of (3.5) is

$$q_o = Q_o e^{-x(L/L_T)} - \frac{B_o e^{-\alpha(1-x)}}{(\alpha + L/L_T)}, \qquad (3.12)$$

where Q_o is an arbitrary constant. (Recall that it is also a function of n.)

To satisfy the boundary conditions on $x = 0$ and Lr_o must be found but from (3.4) this will depend on higher modes (in j) of q, so that r_o will depend on the solution q_2. That solution follows from (3.3),

$$q_2 = C_{2,1}e^{g_{2,1}(x-1)} + C_{2,2}e^{g_{2,2}x} + \frac{L}{\delta_S}\frac{2^{1/2}B_o e^{-\alpha(1-x)}}{(\alpha - g_{2,1})(\alpha - g_{2,2})}, \qquad (3.13)$$

where the two constants

$$g_{j,k} = -\frac{L}{2\delta_S} - (-1)^k\frac{L}{2\delta_S}\left\{1 + 4\left(\frac{\delta_S}{L}\right)^2\left[F(2j-1) + \left(\frac{L}{L_T}\right)^2\right]\right\}^{1/2}, \quad k = 1, 2. \qquad (3.14)$$

The first root is always positive representing decay away from the eastern boundary. When, as in our case, $\delta_S/L \ll 1$, this root is $O(L/L_T)$ for moderate j. This root represents the thermal decay of signals from the eastern boundary on the scale L_T, which, we recall, depends on mode number n. The second root is always negative, decaying from the western boundary, and for $\delta_S/L \ll 1$ is $O(L/\delta_S)$ and so is qualitatively similar to Stommel's mode of the western boundary layer. For very large j both roots approach $F^{1/2}$ and correspond to baroclinic boundary layers whose width is of the order of the deformation radius. Although boundary layer solutions are possible with this problem the possibility of changes in scale for large n and j suggest use of the full solution for all parameter values.

One can see now the crux of the problem. Using the condition that $u_j = 0$ on $x = 0$ and L for each j separately, we can for $j = 0$ determine $C_{2,1}$ and $C_{2,2}$ in terms of B_o and Q_o. However, to satisfy the condition that $u_2 = 0$ at $x = 0$ and $x = 1$, since $q_2 \neq 0$, requires that that we determine r_2. This in turn requires [see (3.4)] the existence of a q_4, and so on. All even j modes will thus be excited whose homogeneous solutions will be of the form for $j > 2$,

$$q_j = C_{j,1}e^{g_{j,1}(x-1)} + C_{j,2}e^{g_{j,2}x}, \qquad (3.15)$$

and with the use of the boundary conditions, each set of constants, $C_{j,1}$ and $C_{j,2}$, are determined in terms of previously determined constants for smaller j each of which ultimately will depend on the two constants Q_o and B_o. In the appendix we list the table of the coefficients $C_{j,1}$ and $C_{j,2}$ in recursive form. Once these coefficients are determined the solutions for r_j can be constructed as well. Although B_o is considered an externally imposed factor, the amplitude of the Kelvin-like solution, Q_o must be determined. A convenient way to do so is to employ the integral condition described in the next section.

4. The integral condition and the determination of Q_o

If (2.5c) is integrated over the entire domain of the problem and the boundary conditions are imposed, we obtain the integral condition,

$$D \int_0^1 dx \int_{-\infty}^{\infty} d\xi(\eta) = -\int_0^1 dx \int_{-\infty}^{\infty} d\xi E, \quad (4.1)$$

or in terms of q and r,

$$\sum_j \int_0^1 dx \int_{-\infty}^{\infty} d\xi (q_j + r_j)\psi_j(\xi) = -2^{3/2}\pi^{1/4}\frac{L}{L_T}B_o\frac{(1 - e^{-\alpha})}{\alpha}, \quad (4.2)$$

where we have used (3.8), that is, that the imposed heating due to mixing is proportional to the first Hermite function. Using standard results from integral tables (e.g., Gradshteyn and Ryzhik 2000) we obtain, as the condition,

$$\sum_{j\text{even}} \int_0^1 dx (q_j + r_j)\frac{j!}{(2^j j!)^{1/2}(j/2)!} = -2\frac{L}{L_T}B_o(1 - e^{-\alpha}). \quad (4.3)$$

With the aid of the coefficients given in the appendix, one can obtain a rather complicated formula for Q_o. The sum on the left-hand side is first evaluated with $Q_o = 1$ and $B_o = 0$ using the recursion relations of the appendix. Call that SumQ. The sum is then recalculated with $Q_o = 0$ to obtain SumB. It then follows that

$$Q_o = \frac{-\text{Sum}B - 2L/L_T B_o(1 - e^{-\alpha})/\alpha}{\text{Sum}Q}, \quad (4.4)$$

and this must be done separately for each n. When Q_o has been so determined the solution is complete and q, r, and v can easily be obtained.

5. Results

For the calculations presented below the coefficient Q has been chosen in the form given by (3.9). The amplitude B_o is, of course, arbitrary in this linear problem and so the *form* of the solution is independent of its value. We frankly choose a value of B_o to obtain currents in the range of those observed. We choose B_o to yield of value of $J = 6 \times 10^{-9}$ s^{-1} corresponding to a maximum value of Q of this order near the eastern boundary. Were this heating balanced entirely by vertical motion (diapycnal velocity in this model), it would give rise to a value of w on the order of 10^{-2}–10^{-3} cm s^{-1}, which is in the range of diapycnal velocity estimated by Sloyan et al. (2002, manuscript submitted to *J. Phys. Oceanogr.*).

Figure 2 shows a contour plot in the y–z plane of the zonal velocity for the case where $\mu = 10$ and $\alpha = 4$ (parameters used in Fig. 1). The cross section is shown at a location half way across the basin; that is, at $x = 0.5$. The thermal decay length L_T has been chosen to be 5 times the basin width. The parameter F has been chosen to be 100 so we have an equatorial region whose longitudinal extent is 10 equatorial deformation radii. This yields a very narrow Stommel boundary layer width $\delta_S/L = 0.002$ and in the figures that follow the flow in that region will not be shown although it is part of the overall solution as calculated; that is, no boundary layer approximation has been made. The solution is represented using 40 vertical modes as well as 40 Hermite functions in latitude. By altering the number of modes maintained we have checked that this number is more than sufficient to properly represent the solution.

In Fig. 2 we see stacked jets, clearly reminiscent of the figures shown in the observational papers referenced in section 1. The horizontal scale of the currents is of the order of the deformation radius but in fact is somewhat smaller than the first deformation radius (one unit in the current scaling), reflecting the contribution made by higher vertical modes to the solution. Figure 3 shows the profile of the zonal velocity versus depth at the equator for the calculation, which was shown in the previous figure. Six jets are shown, three to the east and three to the west. Isolines of the zonal velocity in the

x, y plane are shown in Fig. 4 at the level $z/H = -0.7$ in the region of an eastward jet. There is a smooth deceleration of the flow as the eastern boundary is approached where $u = 0$, and, consistent with the often noted observational fact, there is no sign of a recirculation to close the flow. Instead, as shown in Fig. 5, the flow closes in the vertical plane eastward flow at one level (e.g., $z/H = -0.7$) is perfectly compensated by the reverse flow in the opposite direction at deeper levels. Figure 5c shows the meridional velocity near the western boundary (note the stretched coordinate). The meridional velocity is induced by the local convergence of the zonal velocity and we note that it is limited to within a deformation radius of the equator. This similarly is true near the eastern boundary. The flow, driven by the localized buoyancy forcing is confined to the equatorial band.

As the buoyancy forcing is increasingly limited to the eastern boundary the wavelength in the vertical of the zonal jets decreases. Figure 6 shows the zonal velocity in the case where the exponential decay factor, α, has been increased from 4 to 8. The number of jets has nearly doubled although the jet strength is now weaker. Similar calculations with increasing the vertical decay factor of the forcing will also increase the vertical wavenumber of the jets, although those results are not shown for the sake of brevity.

The solution depends significantly on the parameter $L/L_T(1)$, that is, on the ratio of the basin width to the thermal decay scale of the lowest Kelvin mode. In Fig. 2 that ratio is 0.2. For a basin 12 000 km wide and a value of $c(1)$ of 240 cm s^{-1}, this yields a value of κ of $O(4 \times 10^{-8})s^{-1}$ or a dissipation damping time of about 290 days. If that parameter is increased, that is, if the thermal dissipation is significantly increased the number of jets decreases as the higher modes of the solution become more strongly damped. Figure 7 shows the zonal velocity when the damping scale is 2.5 times shorter than that shown in Fig. 2. Only the lowest mode survives and there are only two jets. Even stronger damping would eliminate those. For lower damping, that is, for smaller values of $L/L_T(1)$, the number of jets increases. However, should $L/L_T(1)$ become very small the jet structure is also eliminated. In this limit information at each z propagates directly westward and there is no penetration. For example we note from (3.5) that in this limit $q_o(n)$ will propagate unchanged outside the forcing region and therefore will maintain the z structure of the forcing for all x. An example is shown in Fig. 8 in the extreme limit $L/L_T(1) = 0.01$. Thus, for moderately small $L/L_T(1)$ the lowest modes propagate directly across the basin without setting the deep ocean in motion, the very high vertical modes are trapped to the region of the forcing and it is the modes of intermediate n which are evident in the deep ocean.

It is a naturally fragile part of this linear theory that the number of equatorial jets does depend on the damping rate about which we can only express great uncertainty. However, the observed ability of equatorial Kelvin and Rossby waves to easily transit the ocean basins leads one to suspect that a moderately small but $O(1)$ value of $L/L_T(1)$ would be plausible.

6. Discussion and summary

The simple, steady linear theory presented here describes the equatorial deep jets as the response to a steady, spatially localized buoyancy forcing, which we suggest is due to mixing at the base of the thermocline, a mixing that has been observed. An attractive feature of the forcing is that the jets appear *below* the level of the imposed forcing. This distinguishes the present theory from earlier work (e.g., Ponte 1989; Wang et al. 1994) in which boundary forcing is required at the depth of the deep jets themselves. The localization of the forcing actually enhances the oscillatory character of the response. The steady forcing due to turbulent mixing at the base of the equatorial thermocline is a permanent feature of the dynamics and the steady response yields deep jets for a range of thermal damping which is plausibly oceanographically appropriate.

A fundamental feature of the solution is the Kelvin wave-like response, that is, that part of the solution represented by the function q_o. The amplitude of that response is coupled to response of higher meridional modes by the integral condition of section 4, a condition that we have found necessary to complete the solution. The integral condition appears necessary to express the mass conservation condition at each level in the equatorial basin and is reminiscent of the dependence of the solution for the midlatitude problem in the treatment by Edwards and Pedlosky (1995) where a similar integral condition is required to complete the solution.

The model presented here has some grave deficiencies. The linear nature of the dynamics and thermodynamics might be plausibly accepted but the external and arbitrary specification of the forcing is a intrinsic weakness. It would be much more pleasing if a model which contained both the nonadiabatic dynamics of the thermocline and the deep jets could be analyzed that exposed the naturally occurring mixing in the model as the driving mechanism for the deep jets. Such a model, nonlinear by its nature is, of course, far beyond the scope of the present analysis which might best be considered as a hypothesis of the "if … then" type. That is, if such mixing providing a buoyancy source is reasonable, then one would expect to see the deep jet response as predicted by the present model.

Acknowledgments

I am particularly grateful to the constructive suggestions of two anonymous reviewers of an earlier version of this paper. This work has been supported in part by a grant from the National Science Foundation OCE 9901654.

REFERENCES

Abramowitz M., and I. Stegun, 1970: *Handbook of Mathematical Functions.* National Bureau of Standards, U.S. Government Printing Office, 1046 pp.

Anderson D. L. T., and P. B. Rowlands, 1976: The role of inertia-gravity and planetary waves in the response of a tropical ocean to the incidence of a Kelvin wave on a meridional boundary. *J. Mar. Res.*, **34**, 295–312. Find this article online

Edwards C. A., and J. Pedlosky, 1995: The influence of distributed sources and upwelling on the baroclinic structure of the abyssal circulation. *J. Phys. Oceanogr.*, **25**, 2259–2284. Find this article online

Firing E., 1987: Deep zonal currents in the central equatorial Pacific. *J. Mar. Res.*, **45**, 791–812. Find this article online

Gill A. E., 1980: Some simple solutions for heat-induced tropical circulations. *Quart. J. Roy. Meteor. Soc.*, **106**, 447–462. Find this article online

Gill A. E., 1982: *Atmosphere–Ocean Dynamics.* Academic Press, 662 pp.

Gradshteyn I. S., and I. M. Ryzhik, 2000: *Table of Integrals, Series and Products.* 6th ed. Academic Press, 1163 pp.

Luyten J. R., and F. C. Swallow, 1976: Equatorial undercurrents. *Deep-Sea Res.*, **23**, 999–1001. Find this article online

McCreary J. P., 1981: A linear stratified ocean model of the Equatorial Undercurrent. *Philos. Trans. Roy. Soc. London*, **A298**, 603–635. Find this article online

Moore D. W., and S. G. H. Philander, 1977: Modeling the tropical oceanic circulation. *The Sea,* E. D. Holdberg, Ed., Marine Modeling, Vol. 6, Wiley and Sons, 319–362.

O'Neill K., and J. R. Luyten, 1984: Equatorial velocity profiles. Part II: Zonal component. *J. Phys. Oceanogr.*, **14**, 1842–1852. Find this article online

Ponte R. M., 1989: A simple model for deep equatorial zonal currents forced at lateral boundaries. *J. Phys. Oceanogr.*, **19**, 1181–1891. Find this article online

Ponte R. M., J. Luyten, and P. L. Richardson, 1990: Equatorial deep jets in the Atlantic. *Deep-Sea Res.*, **37**, 711–713. Find this article online

Wang D., D. W. Moore, and L. M. Rothstein, 1994: Exact solutions to Kawase's linear model of deep ocean circulation. *J. Phys. Oceanogr.*, **24**, 2188–2195. Find this article online

Wunsch C., 1977: Response of an equatorial ocean to a periodic monsoon. *J. Phys. Oceanogr.*, **7**, 497–511. Find this article online

---

APPENDIX

7. Table of Coefficients $C_{j,1}$ and $C_{j,2}$

It is helpful to define the following function:

$$f(j, k) = \left(\frac{j}{j-1}\right)^{1/2}\left[1 + \frac{\delta_S}{L}\left(g_{j,k} + \frac{L}{L_T}\right)\right], \qquad k = 1, 2 \tag{A.1}$$

in terms of which we can determine the $C_{j,1}$ and $C_{j,2}$ as

$$C_{4,2} = \frac{C_{2,1}(e^{g_{2,1}} - e^{g_{4,1}})}{f_{4,2}(1 - e^{g_{4,2}-g_{4,1}})} + \frac{C_{2,2}(1 - e^{g_{2,2}-g_{4,1}})}{f_{4,2}(1 - e^{g_{4,2}-g_{4,1}})} + \frac{B_o 2^{n/2} L/\delta_s (e^{\alpha} - e^{g_{4,1}})}{f_{4,2}(1 - e^{g_{4,2}-g_{4,1}})(\alpha - g_{2,1})(\alpha - g_{2,2})} \quad \text{(A.2d)}$$

for $j > 4$:

$$C_{j+2,1} = \frac{C_{j,1}(1 - e^{g_{j+2,2}-g_{j,1}}) + C_{j,2}(e^{g_{j,2}} - e^{g_{j+2,2}})}{f_{j+2,1}(1 - e^{g_{j+2,2}-g_{j+2,1}})} \quad \text{(A.3a)}$$

$$C_{j+2,2} = \frac{C_{j,1}(e^{-g_{j,1}} - e^{-g_{j+2,1}}) + C_{j,2}(1 - e^{g_{j,2}-g_{j+2,1}})}{f_{j+2,2}(1 - e^{g_{j+2,2}-g_{j+2,1}})}. \quad \text{(A.3b)}$$

(Click the equation graphic to enlarge/reduce size)

Figures

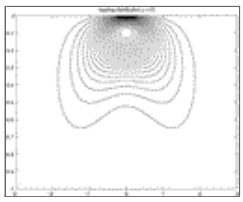

Click on thumbnail for full-sized image.

FIG. 1. A cross section in the y–z plane showing the distribution of the function Q for the case $\mu = 10$. The y variable is scaled with the equatorial deformation radius corresponding to the lowest vertical mode, while z is scaled with the total depth

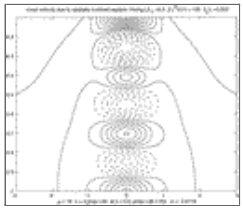

Click on thumbnail for full-sized image.

FIG. 2. A y–z cross section of the zonal velocity for the parameters $\mu = 10$, $\alpha = 4$, $L/L_T = 0.2$. The cross section is shown at $x = 0.5$, i.e., half way across the basin. The magnitudes of the flow are determined by the arbitrary value chosen for the localized buoyancy source

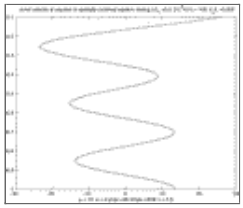

Click on thumbnail for full-sized image.

FIG. 3. A profile of the zonal velocity at the equator for the case described by Fig. 1

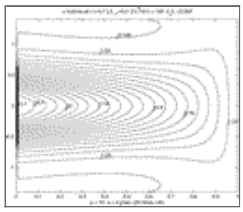

Click on thumbnail for full-sized image.

FIG. 4. The isolines of the zonal velocity at $z/H = -0.7$, in a region of an eastward jet

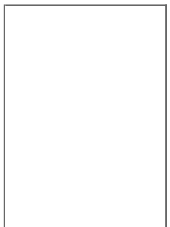

Click on thumbnail for full-sized image.

FIG. 5. The horizontal velocity for the case in Fig. 2: (a) at $z/H = -0.7$, (b) at $z/H = -0.3$, and (c) isolines of the meridional velocity in the vicinity of the western boundary at the same z/H (note the expanded scale in x)

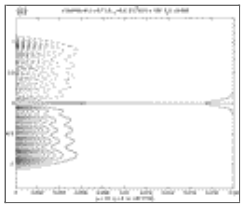

Click on thumbnail for full-sized image.

FIG. 5. (*Continued*)

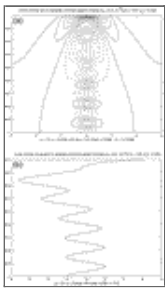

Click on thumbnail for full-sized image.

FIG. 6. As in Fig. 2 for $\alpha = 8$: (a) y–z cross section and (b) profile at the equator

Click on thumbnail for full-sized image.

FIG. 7. The cross section of the zonal velocity for the same parameter settings as Fig. 2 except for $L/L_T = 0.5$: (a) cross section and (b) profile

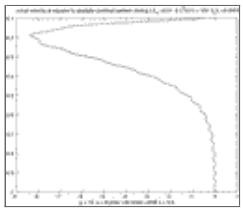

Click on thumbnail for full-sized image.

FIG. 8. The velocity profile at the equator for $L/L_T = 0.01$. Note the absence of deep jets.

* Woods Hole Oceanographic Institution Contribution Number 10639.

Corresponding author address: Dr. Joseph Pedlosky, Woods Hole Oceanographic Institution, Clark 363, MS 21, Woods Hole, MA 02543. E-mail: jpedlosky@whoi.edu

top

Headquarters: 45 Beacon Street Boston, MA 02108-3693
DC Office: 1120 G Street, NW, Suite 800 Washington DC, 20005-3826
amsinfo@ametsoc.org Phone: 617-227-2425 Fax: 617-742-8718
Allen Press, Inc. assists in the online publication of *AMS* journals.